Convective self-aggregation, cold pools, and domain size

Nadir Jeevanjee,[1,2] and David M. Romps,[1,3]

Convective self-aggregation refers to a phenomenon in cloud-resolving simulations wherein the atmosphere spontaneously develops a circulation with a convecting moist patch and a nonconvecting dry patch. All previous studies have found a sharp transition to aggregated convection when the domain size exceeds a critical threshold, typically in the range of 200–300 km. Here, we show that cold pools are responsible for this sharp transition. When cold pools are inhibited, self-aggregation occurs at all domain sizes. In this case, the aggregation strength decreases smoothly as the domain size L is decreased below about 200–300 km. A streamfunction analysis reveals two distinct sources for the air subsiding into the dry-patch boundary layer: a moist, shallow circulation and a dry, deep circulation. The deep circulation scales with L, whereas the shallow circulation does not. At small L, the shallow circulation dominates, thereby weakening the aggregation. **Citation:** Jeevanjee, N., and D. M. Romps (2013), Convective self-aggregation, cold pools, and domain size, Geophys. Res. Lett., 40, doi:10.1002/grl.50204.

1. Introduction

Organized convection, in which the spatial pattern of convection is fixed and persistent over time, has been found in both observations and numerical studies [Houze and Betts, 1981; Grabowski and Moncrieff, 2001; Stephens et al., 2008] and at a wide range of scales. In particular, recent numerical studies [Bretherton et al., 2005; Khairoutdinov and Emanuel (Aggregation of convection and the regulation of tropical climate; preprint: https://ams.confex.com/ams/pdfpapers/168418.pdf); Muller and Held, 2012] with cloud-resolving models (CRMs) have shown that horizontally quasi-homogeneous tropical convection can be unstable, yielding spontaneous development of a circulation featuring a moist, convecting patch and a dry, nonconvecting patch. This self-aggregated state has significantly different horizontal-mean properties than the quasi-homogeneous state from which it formed: it is significantly drier in the mean, for instance, and hence exhibits much stronger mean longwave radiative cooling (LRC). Horizontal variations in LRC are important as well, as differences in LRC between moist and dry columns play a critical role in the feedbacks responsible for self-aggregation; see Bretherton et al. [2005] and Muller and Held [2012] for details.

These two papers also investigated the sensitivity of aggregation to various parameters, one of these being the domain size L. Both studies found that quasi-homogeneous states will only self-aggregate if L & 200–300 km. The goal of this paper is to shed light on this domain-size dependence.

This work is motivated by the routine use of CRMs as a benchmark in the evaluation of convective parameterizations for global climate models. To improve the realism and statistics of CRM simulations, modelers have typically preferred the use of larger domains. Self-aggregation, however, presents a catastrophic failure of CRMs to converge as a function of domain size, casting doubt on the reliability of CRMs as a benchmark.

2. Numerical Simulations

All simulations in this paper were performed using Das Atmosphärische Modell (DAM) [Romps, 2008]. DAM is a three-dimensional, fully compressible, nonhydrostatic CRM that uses the six-class Lin-Lord-Kreuger microphysics scheme. For this paper, we performed runs on both three-dimensional (3-D) square domains as well as effectively two-dimensional (2-D) bowling-alley domains, all of various sizes. All domains were doubly periodic with a horizontal grid spacing of 3 km, and simulations were run over a nondynamical ocean with a fixed sea-surface temperature (SST) of 301 K. This choice of SST is typical of the tropical oceans and is the same as that used in Bretherton et al. [2005]. It is also squarely in the range of SSTs shown to be conducive to aggregation in Khairoutdinov and Emanuel [2010]. Surface enthalpy fluxes were calculated using a bulk aerodynamic formula, and interactive shortwave and longwave radiative fluxes were calculated using RRTM.

Each run was 60 days long and was initialized with an aggregated distribution of water vapor similar to that used in Muller and Held [2012]. Here, the lowest-level specific humidity q started at 16 g/kg in the center of the domain and decreased to 8 g/kg at the edge, and this horizontal distribution decreased exponentially with height with a scale height of 3 km. The initial horizon- tal q distribution was a radial function for the square domains and was linear along the long dimension in the bowling-alley domains. The initial temperature profile was obtained from a small-domain (i.e., non-aggregated) sim- ulation of radiative-convective equilibrium. We turned off large-scale dynamical forcings, set initial horizontal winds to zero, and nudged the horizontal-mean winds to zero over a time scale of two hours, both for consistency with previous work [Muller and Held, 2012; Bretherton et al.,

[1]Earth Sciences Division, Lawrence Berkeley National Laboratory, Berkeley, CA, USA.
[2]Department of Physics, UC Berkeley, Berkeley, CA, USA.
[3]Department of Earth and Planetary Science, UC Berkeley, Berkeley, CA, USA.

Corresponding author: N. Jeevanjee, Department of Physics, University of California at Berkeley, Berkeley, CA 94702, USA. (jeevanje@berkeley.edu)

2005] and because we found these adjustments conducive to aggregation.

3. Aggregation in 3-D

As a first task, we reproduced the phenomenon of convective self-aggregation in 3-D, as well as its critical dependence on domain size. Figure 1 shows x-y snapshots of specific humidity q on day 60 at z = 500 m for various domain sizes L. Aggregation, with its trademark dry patches in regions of steady-state subsidence, is clearly evident for domain sizes larger than L "" 300 km. This is in rough agreement with the critical domain size of 200–300 km found in Bretherton et al. [2005] and Muller and Held [2012].

To investigate the role of the boundary layer (BL) in convective aggregation, we eliminated cold pools by turning off low-level (z < 1000 m) evaporation of precipitation. We chose z = 1000 m for the evaporation cutoff height simply because it seemed sufficiently high enough to kill the cold pools. Lowering the cutoff height from 1000 to 600 m was enough to reintroduce cold pools. In this no-cold-pool scenario, we found that self-aggregation occurs at all domain sizes but gradually decreases in strength as the domain size L decreases. This can be seen in Figure 2, which plots the same quantities as Figure 1 for the simulations with no cold pools. It appears that cold pools are responsible for inhibiting convective aggregation in small domains and for generating a discontinuous dependence of self-aggregation on domain size.

As stated above, our goal is to explain the development of convective aggregation at a characteristic domain size of 200–300 km. Since cold pools neither generate nor maintain convective self-aggregation, it is natural to study self-aggregation in their absence. Although self-aggregation is a continuous function of domain size in the absence of cold pools—as opposed to discontinuous with cold pools—our working hypothesis is that the underlying physics of self-aggregation is the same in both cases. Furthermore, as a practical matter, it is easier to diagnose the mechanisms responsible for a continuous transition than for a discontinuous one.

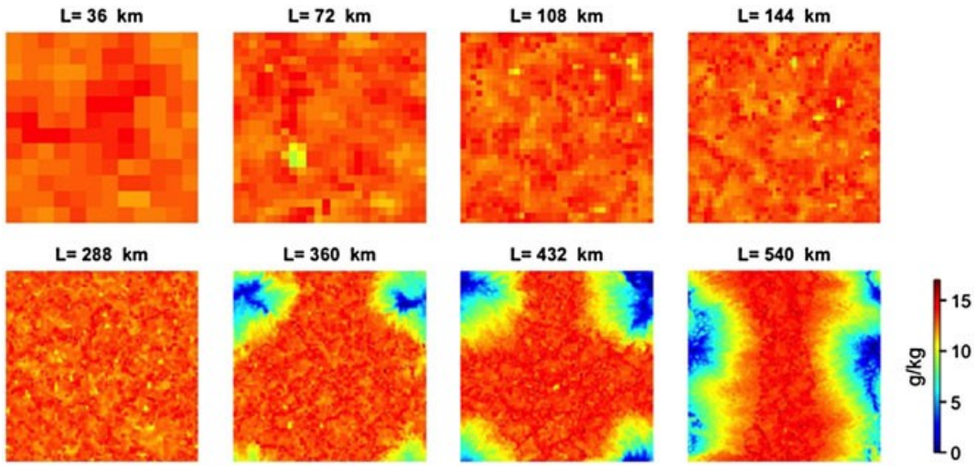

Figure 1. Horizontal specific-humidity distribution [g/kg] at z = 500 m on day 60 for various domain sizes L in the presence of cold pools. Note the sharp transition to an aggregated state between L = 288 and L = 360 km.

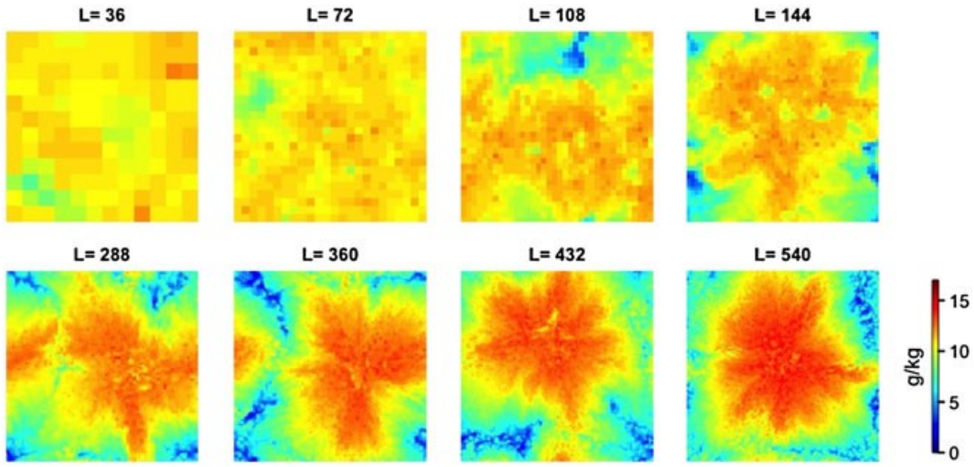

Figure 2. Same as Figure 1 but in the absence of cold pools. Note that, in contrast to Figure 1, aggregation occurs at domain sizes less than 300 km and only gradually weakens as L decreases.

4. Aggregation in 2-D

To facilitate the analysis of the domain-size dependence of self-aggregation, we performed a suite of similar 60 day runs over a bowling-alley domain where the long domain edge (along the x axis) varied and the short domain edge (along the y axis) was fixed at 12 km. We averaged over y, yielding what were effectively 2-D runs, which were then amenable to streamfunction analysis and study of the steady-state circulation. The setup of the simulations was identical to that of the full 3-D runs above except for the domain dimensions. Steady-state values of variables were obtained by averaging over the last 20 days of each run. Boundary-layer averages were also employed, where the height h of the BL is defined by the height z at which $d^2()/dz^2$ is a maximum, where () is the steady-state potential temperature and z is restricted to 200 m < z < 4000 m. For unaggregated domains the ()(z) profile is obtained by horizontally averaging () over the whole domain. For aggregated domains, however, the ()(z) profile is obtained by horizontally averaging over only the driest 10% of columns, since the BL height is lowest there due to the large-scale subsidence over those columns.

We first performed simulations with cold pools. The left-hand panel of Figure 3 shows horizontal profiles of steady-state q, averaged from z = 0 to h. Aggregation is evident for domain sizes bigger than L "" 250 km, again in agreement with a critical domain size in the 200–300-km range.

We then performed these runs without cold pools, as in the previous section. The results are shown in the right-hand panel of Figure 3. Note the gradual, but pro- nounced, increase in aggregation strength as L increases towards 200 km, similar to that of the 3-D runs in Figure 2. This shows that the 2-D and 3-D phenomena are quite anal- ogous, so studying the 2-D case should provide insight into the 3-D case. We perform streamfunction analyses of our 2-D runs in the next section.

5. Streamfunction Analysis

We begin by plotting the steady-state water-vapor distribution and streamfunction contours for a few representative cases in Figure 4. The streamfunction may be naturally divided into a shallow circulation (confined below z ≈ 3500 m) and a deep circulation (extending above z ≈ 3500 m). Note that a secondary shallow circulation was also observed in Bretherton et al. [2005] and Muller and Held [2012]. The contour spacings for each plot in Figure 4 are chosen so that each plot has the same number of contour lines. Note that the number of deep convection contours increases with L, implying that the magnitude of the deep circulation relative to that of the shallow circulation increases as L increases. We check this by plotting the magnitudes of these circulations as functions of L in Figure 5. We take S to be the difference between the low-level streamfunction maximum C and the maximum value of the streamfunction along the z = 3500 m contour. We then take D to be the maximum value of the streamfunction along the z = 3500 m contour, so that D + S = C.

Figure 5 confirms that the ratio of D to S grows as L increases: the shallow circulation S varies by only about 50% as L ranges from 72 to 540 km, whereas D varies almost perfectly linearly with L. Thus, D scales with L whereas S does not, and we contend that this is the root cause of the observed domain dependence of aggregation: S dominates at small domains, moistening the dry region and weakening aggregation. More precisely, if we consider the half of the dry region between x = 0 and the x-value of the low-level streamfunction maximum, then C is the magnitude of the circulation feeding the BL of this half. The average specific humidity q_C of the air subsiding into this region will be a weighted sum of contributions from S and D, which have characteristic specific humidities $q_S > 0$ and q_D "" 0. Since D is the only quantity in q_C that scales with L, q_C will increase as L decreases.

To assess the length scales over which this transition occurs, we calculated the minimum values q_{min} of the steady-state BL humidity distributions in the right-hand panel of Figure 3. These values are shown in Figure 6 as a function of domain size L. It is apparent that q_{min} approaches an asymptotic value at a characteristic domain size of 200–300 km, just where the critical domain size lies in the simulations that include cold pools.

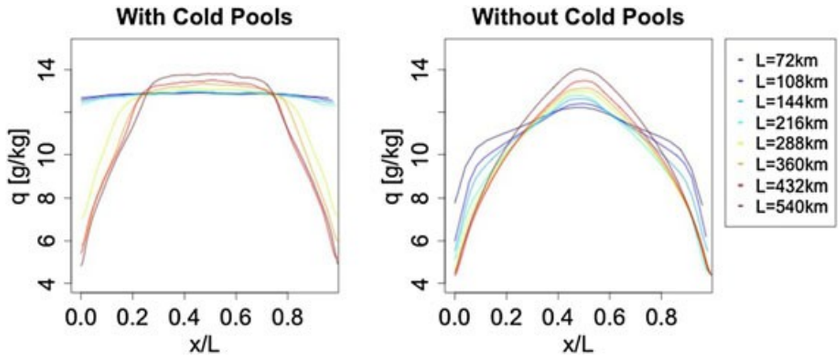

Figure 3. Left-hand panel: Steady-state BL specific humidity q for 2-D runs of various L with cold pools. Note the sharp transition from constant to unimodal humidity between L = 216 and L = 288 km, analogous to the 3-D results in Figure 1. Right-hand panel: Same as left-hand panel but without cold pools. Note the existence of aggregation below the threshold exhibited in the left-hand panel and the gradual weakening of aggregation as L decreases, analogous to the 3-D results in Figure 2.

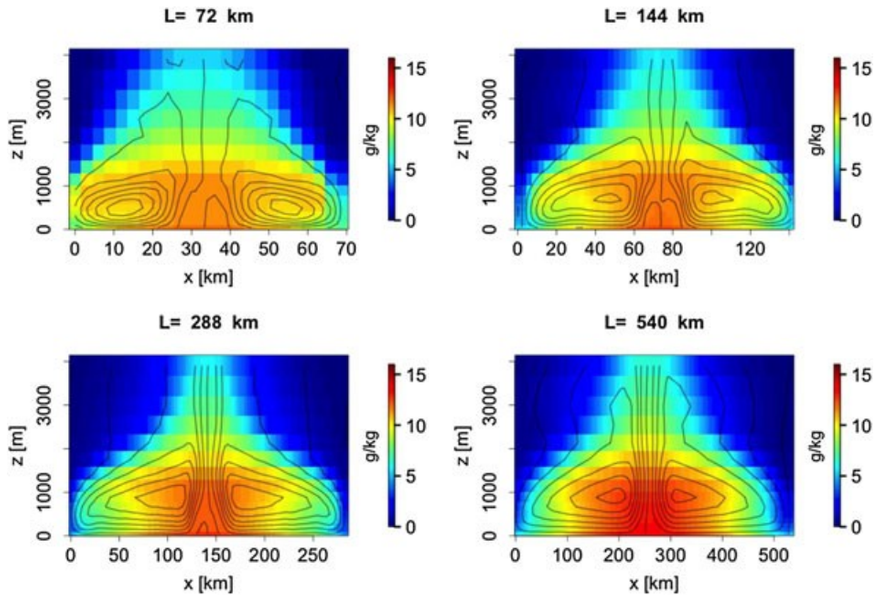

Figure 4. Steady-state specific humidity q overlaid with streamfunction contours for 2-D runs without cold pools for domains with L = 72, 144, 288, and 540 km. The contour spacings are constant within each plot and are 100, 125, 175, and 275 kg/m/s, respectively. These values are chosen so that each plot has the same number of contour lines. In each plot, the circulation around the streamfunction maximum consists of a shallow circulation confined to z ˗ 3500 m, as well as a deep circulation that extends above z "" 3500 m. Note that the number of deep convection contours increases with L, implying that the magnitude of the deep circulation relative to that of the shallow circulation increases as L increases.

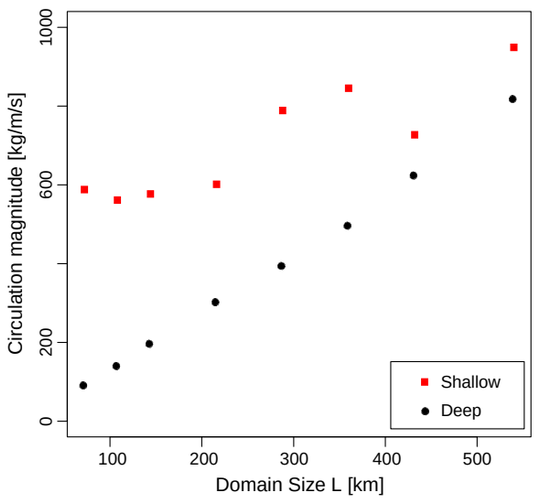

Figure 5. Circulation magnitudes as a function of domain size L. The magnitude D of the dry, deep circulation is given by the black dots, while the magnitude S of the humid, shallow circulation is given by the red squares. Note that D varies linearly with L, whereas S varies by only ~ 50%. Therefore, at small L, the shallow circulation dominates, moistening the dry region and weakening aggregation.

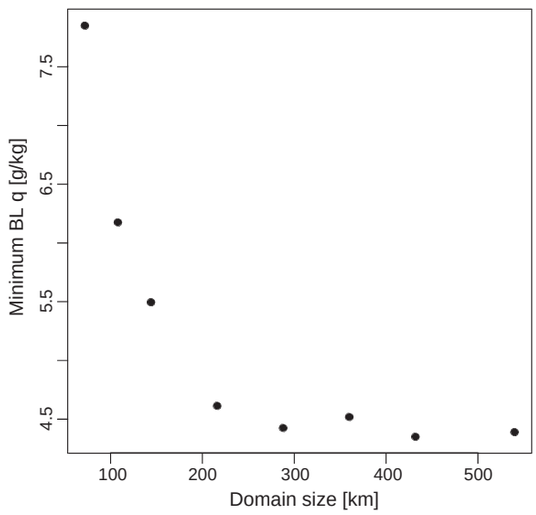

Figure 6. Aggregation strength, as measured by the minimum BL specific humidity q_{min}, plotted as a function of domain size L. Note that q_{min} approaches its asymptotic value at a characteristic domain size of 200–300 km, which is where the critical domain size lies in the simulations with cold pools.

6. The Effect of Cold Pools on Aggregation

The analysis of the previous section explains why aggregation gradually weakens as L decreases in our no-cold-pool simulations but does not address how or why cold pools inhibit aggregation below the critical domain size. To investigate this, we performed a 2-D simulation with L = 216 km with initial conditions given by the day 60 snapshot of our earlier L = 216 km no-cold-pool run; this gave our run an initial aggregated water-vapor distribution

similar to that shown for L = 216 km in the right panel of Figure 3. For this new run, we turned the cold pools back on and watched the convection disaggregate. We found that the boundary layer in the dry region becomes fully moistened by about day 11, whereas the lower and upper troposphere do not fully moisten until about day 17. This points to a sequence of events whereby the cold pools first moisten the dry-patch boundary layer, followed by deepening convection that moistens the free troposphere. The larger the domain, the drier the boundary layer in the dry patch and the longer the distance the cold pools must travel to bring moisture there. Both of these effects prevent the cold pools from homogenizing moisture and convection above the observed critical domain size.

Acknowledgments. This work was supported by the U.S. Department of Energy's Earth System Modeling, an Office of Science, Office of Biological and Environmental Research program under Contract No. DE-AC02-05CH11231.

References

Bretherton, C. S., P. N. Blossey, and M. Khairoutdinov (2005), An energy-balance analysis of deep convective self-aggregation above uniform SST, J. Atmos. Sci., 62(12), 4273–4292, doi:10.1175/JAS3614.1.

Grabowski, W. W., and M. W. Moncrieff (2001), Large-scale organization of tropical convection in two-dimensional explicit numerical simulations, Q. J. R. Meteorol. Soc., 127 (572), 445–468, doi:10.1002/qj.49712757211.

Houze, R. A., and A. K. Betts (1981), Convection in gate, Rev. Geophys., 19(4), 541–576.

Muller, C. J., and I. M. Held (2012), Detailed investigation of the self-aggregation of convection in cloud-resolving simulations, J. Atmos. Sci., 69(8), 2551–2565, doi:10.1175/JAS-D-11-0257.1.

Romps, D. M. (2008), The dry-entropy budget of a moist atmosphere, J. Atmos. Sci., 65(12), 3779–3799, doi:10.1175/2008JAS2679.1.

Stephens, G. L., S. van den Heever, and L. Pakula (2008), Radiative-convective feedbacks in idealized states of radiative-convective equilibrium, J. Atmos. Sci., 65(12), 3899–3916, doi:10.1175/2008JAS2524.1.